Proceedings of the Canadian Society for Mechanical Engineering International Congress
32nd Annual Conference of the Computational Fluid Dynamics Society of Canada
Canadian Society of Rheology Symposium
CSME-CFDSC-CSR 2025
May 25–28, 2025, Montréal, Québec, Canada

Characteristics of Combustion and NOx Emissions of Ammonia/Methane flames in a premixed swirl gas turbine combustor

Medhat A. Nemitallah[a,b,*], Mohammed El-Adawy[a]
[a]Interdisciplinary Research Center for Hydrogen Technologies and Carbon Management (IRC-HTCM), King Fahd University of Petroleum & Minerals, Dhahran 31261, Saudi Arabia
[b]Aerospace Engineering Department, King Fahd University of Petroleum & Minerals, Dhahran, Saudi Arabia1
* medhatahmed@kfupm.edu.sa

Abstract—This study employs numerical simulations to investigate the combustion and emission attributes of ammonia/methane (NH_3/CH_4) blends in a swirl burner, utilizing advanced modeling approaches to support their potential industrial application. The chemistry of the combustion process is comprehensively addressed utilizing a detailed mechanism featuring 356 reaction steps and 59 species, integrated within the flamelet generated manifold (FGM) model framework. Raising the NH_3 content from 20% to 80% at a fixed equivalence ratio (φ) of 0.93 leads to a 4.3% reduction in the peak temperature. As the proportion of CH_4 increases, NH_2 radical concentrations decrease while OH radical concentrations rise resulting in enhanced conversion of NH_2 to NO and greater thermally dominated NOx emissions. Increasing ammonia concentration from 20% to 30%, the recorded NOx emissions, comprising NO, N_2O, and NO_2, escalated from 3975 PPM to 4638 PPM, indicating a 14.28% rise. The peak NOx levels were detected when the ammonia concentration reached 30% at φ=0.85. In the NH_3/CH_4 combustion, NO_2 formation is minimal, whereas the contribution of N_2O is significant at higher equivalence ratios, and NO is dominant.

Keywords: NH_3/CH_4 combustion; Clean combustion; Numerical combustion; FGM model; Gas turbine burner

1. INTRODUCTION

The pressing need to address climate change and meet stringent global emissions standards has accelerated the search for sustainable energy alternatives, driving advancements in both scientific research and industrial applications [1, 2]. This transition is fueled by the critical goal of mitigating the adverse effects of carbon-intensive fuels, which significantly contribute to global warming, air pollution, and economic challenges [3]. Among emerging alternatives, ammonia (NH_3) has gained attention as a potential fuel for gas turbines and energy systems, though its adoption requires overcoming technical and environmental challenges, particularly regarding NOx emissions [4].

Ammonia combustion typically generates NOx due to high temperatures and its inherent nitrogen content [5]. Lee et al. [6] observed that while ammonia's lower combustion temperature reduces NOx formation, this benefit is offset by increased NOx production from its nitrogen content. These emissions pose environmental hazards, emphasizing the need for advanced combustion technologies. Gas turbines, traditionally optimized for hydrocarbons like natural gas and diesel, require significant redesigns to accommodate ammonia's distinct properties, including its lower flammability and higher ignition energy. Innovations may include enhanced mixing techniques, new materials, or novel combustion chamber geometries to ensure efficient and stable operation [7]. Kobayashi et al. [8] demonstrated the feasibility of ammonia in gas turbines, with studies exploring swirling flows to stabilize its combustion [9].

Combining ammonia with other fuels, such as hydrogen [10], methane [11], or n-heptane [12], has emerged as a viable strategy to improve combustion stability and efficiency. Such blends reduce CO_2 emissions while leveraging the synergistic effects of hydrocarbons to enhance ammonia's combustion characteristics. Studies indicate that ammonia/methane blends exhibit prolonged ignition delay times compared to pure methane, influenced by blend composition and equivalence ratios. For instance, Valera et al. [13] demonstrated stable combustion with minimal NOx emissions in tangential swirl

combustors, though operational ranges required equivalence ratios exceeding 1. Zitouni et al. [14] found that blending ammonia with methane or hydrogen increases reaction rates by approximately 20%, primarily through reduced activation energy. Methane contributes to linear increases in flame speed and generates OH and CH radicals, while hydrogen has an exponential impact and enhances NH_2 formation from ammonia.

In conclusion, ammonia, a carbon- and sulfur-free energy carrier, shows promise as a substitute fuel in heat engines and a hydrogen carrier. However, its adoption is hindered by limited research into its combustion dynamics and NOx emission characteristics, particularly in industrial furnaces and gas turbine burners. A comprehensive understanding of ammonia's flame behavior and emissions is crucial for its integration into clean energy systems. This study introduces a novel numerical investigation of methane/ammonia combustion near ammonia's lean flammability limit, utilizing the Flamelet Generated Manifold (FGM) approach in CFD. This method offers detailed insights into flame dynamics and emissions under critical conditions, advancing cleaner fuel technology development.

2. NUMERICAL METHODS

2.1 Combustor model and operating conditions

The combustor configuration, illustrated in a two-dimensional (2D) schematic in **Figure 1**, is designed for computational analysis. The combustion chamber is housed within a quartz tube, measuring 30 cm in length, with an internal diameter of 76 mm and a wall thickness of 6 mm. A 10-mm-thick metallic plate is positioned at the base of the combustor to enclose the combustion zone, featuring a centrally located conical structure. This conical element has an outer diameter of 9.5 mm and an inclination angle of 28 degrees. Upstream of the burner inlet, a swirler assembly with eight vanes set at a 45-degree angle facilitates flow dynamics.

The study investigates premixed flames of ammonia/methane/air mixtures under swirling conditions, examining seven distinct cases, denoted as Cases 1 through 7, varying according to the NH_3/CH_4 ratio and the equivalence ratio (φ) as specified in Table 1. Cases 1 and 7 featured different fuel blends with NH_3 and CH_4 compositions of 20% & 80%, and 80% & 20% respectively, at φ of 0.93. Cases 2 and 6 had NH_3 and CH_4 compositions of 30% & 70%, and 70% & 30% respectively, at a global φ of 0.85. Cases 3 and 5 had NH_3 and CH_4 compositions of 40% & 60%, and 60% & 40% respectively, at an equivalence ratio of 0.80. Case 4 consisted of a 50% NH_3 and 50% CH_4 mixture at φ of 0.73. All cases were established under fuel-lean conditions to replicate typical gas turbine combustor flames. The calculation of the fuel's mean mixture fraction (MMF_{fuel}) was carried out using the methodology described in Equation (1) [15]. This calculation was essential for assessing the impact of alterations in fuel composition, particularly the percentage of ammonia, on the dynamics of combustion. By quantifying the mean mixture fraction of the fuel, the study provides a detailed understanding of how varying levels of NH_3 in the fuel mixture affect combustion behavior, including temperature profiles, flame stability, and emission characteristics.

$$MMF_{fuel} = \frac{\dot{m}_{NH_3}+\dot{m}_{CH_4}}{\dot{m}_{NH_3}+\dot{m}_{CH_4}+\dot{m}_{air}} \quad (1)$$

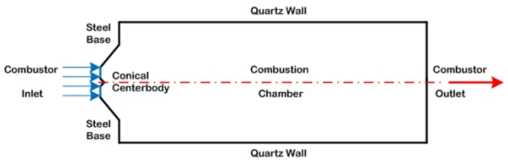

Fig. 1. A 2D schematic representation of the swirl-stabilized model gas turbine combustor.

2.2 Flamelet generated manifold model

The Flamelet Generated Manifold (FGM) model conceptualizes turbulent flames as ensembles of laminar flamelets, with each flamelet representing a localized equilibrium state. This approach utilizes manifold mapping to capture the evolution of turbulent flames in a reduced-dimensional space defined by the mixture fraction and progress variable. By simplifying the representation of chemical kinetics and turbulence-chemistry interactions, the FGM model provides a computationally efficient framework for modeling complex reacting flows. Its ability to accurately predict flame structures and pollutant emissions has made it widely applicable in various domains, including industrial combustion, environmental systems, and propulsion technologies. Detailed information on the FGM model is provided in Reference [16].

2.2 Boundary conditions and calculation methods

The standard k-ε model is used for turbulence simulations, incorporating rotation and curvature effects for improved turbulent viscosity predictions. Renowned for its accuracy in swirling flow velocity fields, it is widely used

in combustion flow modeling [17]. The simulation employs a steady-state, pressure-based solver with gravitational effects considered. The SIMPLE algorithm handles pressure-velocity coupling, and a second-order upwind scheme discretizes all variables. Convergence requires residuals below 10^{-6}. Boundary conditions include mass flow inlets with specified fuel fractions and a pressure outlet. The core body and steel surfaces are modeled as no-slip and adiabatic, while the quartz tube is treated as a semitransparent boundary, enabling convective and radiative heat transfer with a coefficient of 20 W/m²K and an external temperature of 300 K.

Table 1
The operating conditions for premixed swirl flames of blended fuels.

Case	NH_3:CH_4 (%vol)	$\dot{m}_{air}$ (g/s)	$\dot{m}_{NH3}$ (g/s)	$\dot{m}_{CH4}$ (g/s)	MMF	φ_g
1 #	20:80	2.586	0.034	0.128	0.05895	0.93
2 #	30:70	2.586	0.04766626	0.111221274	0.057884898	0.85
3 #	40:60	2.586	0.065038558	0.097557836	0.059156155	0.8
4 #	50:50	2.586	0.085	0.08	0.059978	0.73
5 #	60:40	2.586	0.118195071	0.078796714	0.070784178	0.8
6 #	70:30	2.586	0.163842092	0.070218039	0.082998277	0.85
7 #	80:20	2.586	0.232354213	0.058088553	0.100972899	0.93

3. RESULTS AND DISCUSSIONS

3.1 Numerical model validation

The simulation results were validated by comparing them with findings from Dániel Füzesi et al. [16], demonstrating the accuracy of the numerical approach for swirl flame combustion analysis. Temperature, a key parameter influencing combustion behavior, was examined through radial temperature distributions for a 50:50 NH_3:CH_4 blend (v/v %) at 20 mm above the burner tip, as shown in Figure 2. The results, based on Okafor's chemical kinetic mechanism [18] with 59 species and 356 reactions, showed strong agreement with Füzesi et al.'s data, confirming the reliability of the reaction mechanism for broader combustion applications.

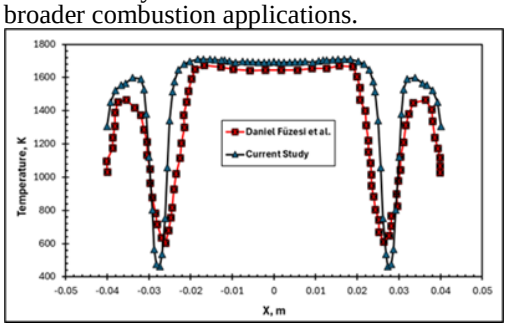

Fig. 2. Radial temperature distribution for the current study and the study of D´aniel Füzesi et al. [16].

3.2 Flow/flame interactions

Figure 3 illustrates the velocity field and streamlines for the simulated cases, providing a detailed depiction of the V-shaped flame, flow dynamics, and the characteristic inner and outer recirculation zones (IRZ and ORZ). The large IRZ is observed to direct the flow toward the combustor wall, significantly affecting flame positioning and temperature distribution. Two key observations emerge from the figure: first, the air mass flow rate remained constant, ensuring uniform axial velocity profiles across all cases; second, variations in the ammonia doping ratio had minimal impact on the size or location of the recirculation zones, aligning with findings from previous studies [19].

Figure 4 shows temperature distributions for the seven cases, highlighting the V-shaped flame typical of swirling combustion. The flame is predominantly situated near the combustor wall, with temperatures decreasing toward the chamber center, influenced by the combustor geometry and the swirling flow. This flame positioning near the liner has been reported in earlier research [19, 20] and is largely attributed to the swirling motion induced by the air swirler. Elevated temperatures at the liner walls raise concerns about thermal stress, reduced structural integrity, and increased maintenance costs.

Variations in peak temperatures between Case 1 and cases with higher ammonia content are attributed to differences in the combustion properties of methane and ammonia. Methane exhibits greater reactivity and combustion efficiency, resulting in higher flame temperatures in methane-dominant scenarios like Case 1. In contrast, higher ammonia concentrations lead to reduced reaction rates and heat release rates (NHRR), causing lower peak

temperatures, as confirmed by prior studies [19, 21].

Flame temperature, a critical factor for stability, depends on airflow, fuel energy release, and heat redistribution. Comparisons between Cases 1 and 7, which share the same equivalence ratio but differ in ammonia content, show a 4.3% reduction in maximum temperature for the higher ammonia case. Similarly, temperature reductions of 2.6% and 1.3% were observed for Cases 2 and 6, and Cases 3 and 5, respectively. This trend is linked to the interaction between ammonia doping levels and the NHRR. As ammonia content increases, its higher heat capacity reduces flame speed and adiabatic temperature, resulting in lower peak temperatures. The heat generated is absorbed by ammonia molecules, shifting the NHRR peak to regions of lower temperature. This mechanism underscores the significant impact of ammonia doping on combustion behavior and temperature profiles in the combustor.

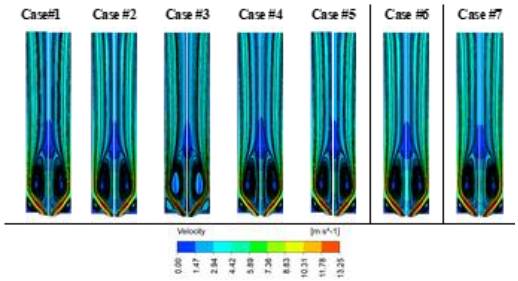

Fig. 3. Velocity fields over ranges of NH_3/CH_4 and equivalence ratios.

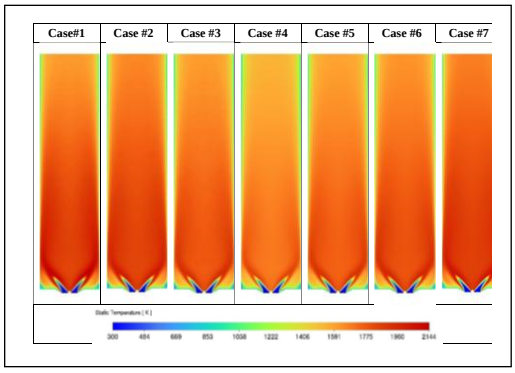

Fig. 4. Temperature contour over ranges of NH_3/CH_4 and equivalence ratios.

3.3 Production of hydroxyl radical (OH)

The hydroxyl radical (OH) is a key intermediate in combustion, particularly within flames, where its concentration reflects both combustion kinetics and flame structure. Figure 5 presents the simulated OH mass fraction distribution at the base of the combustion chamber. The formation of OH and its excited state, OH*, primarily occurs via two dominant pathways:

Reaction (1): $CH + O_2 \rightarrow CO + OH^*$

Reaction (2): $H + O + M \rightarrow OH^* + M$

Reaction (1) becomes increasingly significant with higher methane (CH_4) concentrations, while Reaction (2), though independent of the fuel type, is less probable under atmospheric conditions due to its trimolecular nature. Since the Okafor mechanism does not include OH*, the simulation only represents OH distribution.

The data in **Figure 5** show that increasing the ammonia content in the fuel mixture decreases OH concentrations in the primary combustion zone. This reduction reflects a slower reaction rate, resulting in lower local temperatures. The decline in OH is attributed to the reduced methane content, which is a primary source of OH. Furthermore, ammonia addition enhances OH consumption, contributing to the observed decrease in its concentration.

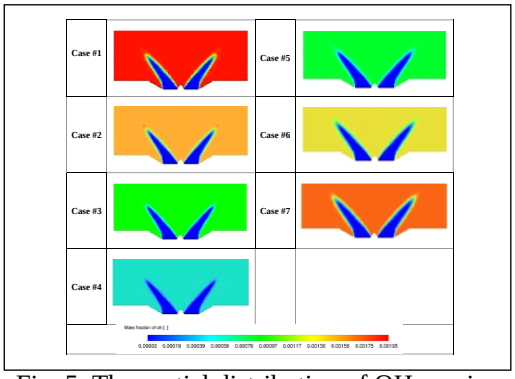

Fig. 5. The spatial distribution of OH species within the combustion chamber over ranges of NH_3/CH_4 and equivalence ratios.

3.4 Production of HNO species

Figure 6 illustrates the mass fraction distribution of the HNO species, highlighting its critical role in NOx formation during the lean combustion of ammonia/methane fuel blends. In this combustion context, the OH and HNO radicals act as key intermediates, driving the oxidation of NH_2 and NH species into NO via the HNO pathway [22]. Unlike OH, the concentration of HNO increases markedly with the addition of ammonia to the fuel mixture. This trend reflects the complex chemical interactions within the combustion process and emphasizes the importance of understanding species-specific behavior.

A detailed comparison of temperature profiles with OH and HNO distributions in Figure 6 reveals that the flame zone exhibits the highest concentrations of both radicals. These

concentration gradients highlight the dynamic chemical reactions occurring within the flame, where OH and HNO play prominent roles. Notably, the levels of these radicals significantly influence the overall NOx emissions in the combustor.

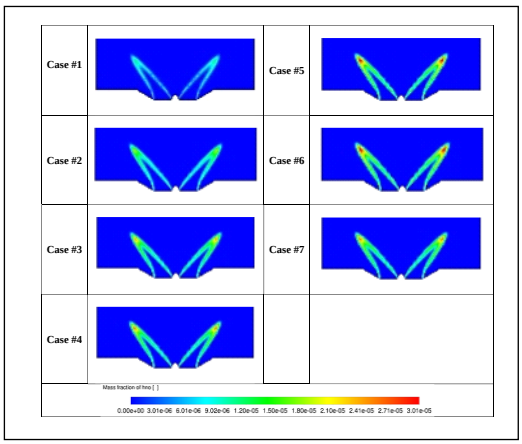

Fig. 6. The spatial distribution of HNO species within the combustion chamber over ranges of NH_3/CH_4 and equivalence ratios.

3.5 NOx emissions

Figure 8 illustrates the peak mass fraction distribution of critical species, including NH_2 and total NOx (comprising NO_2, N_2O, and NO), within ammonia/methane combustion for various operating conditions. This analysis is pivotal in understanding the pathways leading to NOx formation during combustion. The conversion of ammonia into NO and NO_2 involves a series of sequential reactions. Initially, OH radicals facilitate the dehydrogenation of ammonia, yielding NH_2, which subsequently dehydrogenates to form NH. The NH species then reacts with oxygen to produce HNO and atomic oxygen, NO and HO_2, or NO and OH, all contributing to NO formation. NO is further oxidized to NO_2 through reactions with HO_2, while NO_2 can revert to NO via reactions with H and NH_2 radicals [11]. Similarly, the oxidation of methane involves a stepwise transformation: methane (CH_4) converts into methyl radicals (CH_3), which then form formaldehyde (CH_2O), followed by formyl radicals (HCO), carbon monoxide (CO), and ultimately carbon dioxide (CO_2) [11].

The mechanisms governing the oxidation of carbon and nitrogen compounds proceed through distinct pathways, with NOx production relying heavily on ammonia oxidation. In ammonia/methane mixtures, ammonia predominantly oxidizes through high-temperature branching reactions involving H_2/O_2, such as ($H + O_2 \rightarrow OH + O$) and ($H_2O + O \rightarrow 2OH$). Consequently, both carbon species like HCO and nitrogen species like HNO, NO_2, and NH_2 contribute to the formation of OH and HO_2 radicals, which influence the oxidation dynamics. The rates at which radicals are consumed provide further insight into the interactions within these pathways. Notably, the reaction $NH_3 + OH \rightarrow NH_2 + H_2O$ is significantly faster than $CH_4 + OH \rightarrow CH_3 + H_2O$, indicating ammonia's higher tendency to consume OH radicals produced predominantly during methane oxidation [23]. The oxidation of CH_4 is a crucial source of radicals, and as methane's proportion increases, NH_2 radical levels decrease (see Figure 13a), while OH radicals become more prevalent. Higher OH concentrations enhance the conversion of NH_2 to NO while suppressing NO-reducing reactions such as $NH_2 + NO \rightarrow N_2 + H_2O$ and $NH_2 + NO \rightarrow NNH + OH$. This dynamic underscores that introducing methane into an ammonia/methane blend drives NH_2 radicals toward NO formation rather than alternative pathways. The likelihood of NH_2 converting to NO increases with rising OH concentrations, regardless of the ammonia content or NH_2 levels. This highlights the pivotal role of OH radicals in NOx production when ammonia/methane mixtures are used. Even low ammonia levels can significantly elevate NOx emissions, as observed in (Case 2), where the maximum NOx concentration rose by 14.28% when ammonia's proportion increased from 20% (Case 1) to 30% (Case 2). Across all cases studied, the highest NOx concentrations, comprising NO, NO_2, and N_2O, occurred at an ammonia concentration of 30% and an equivalence ratio of 0.85. Interestingly, the results suggest that NO_2 formation is minimal in ammonia/methane combustion, while N_2O contributes substantially to NOx levels. Despite this, NO remains the dominant nitrogen oxide, presenting a major challenge for environmentally sustainable ammonia combustion. The low levels of NO_2 indicate its limited role in total NOx emissions. However, the significant presence of N_2O, a potent greenhouse gas, poses a concern as it can further decompose into NO, exacerbating NOx emissions at higher equivalence ratios.

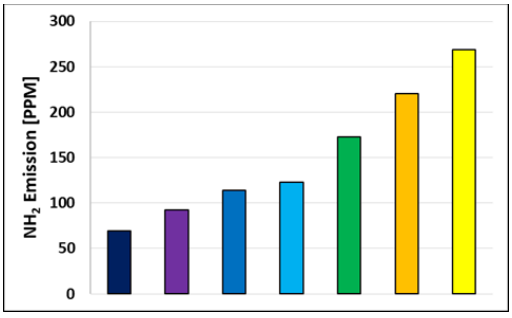

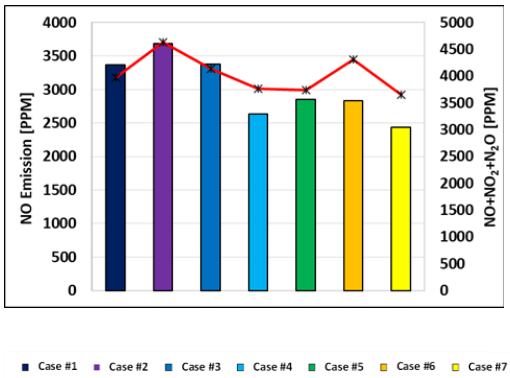

Fig. 8. Maximum mass fractions of NH_2, NO_2, N_2O, and NO over ranges of NH_3/CH_4 and equivalence ratios.

4. CONCLUSIONS

Numerous significant findings emerge from this study as follows:

- The temperature profile indicates that the flame primarily forms near the combustor wall, with a gradual decrease in temperature toward the chamber's center. This behavior highlights the substantial influence of the air swirler's induced swirl on the flame's positioning within the combustor.
- As the proportion of NH_3 in the flame increases, the reaction rate generally diminishes, resulting in a reduced heat release rate and lower maximum temperatures.
- As the CH_4 proportion increases in an ammonia/methane blend, NH_2 radical concentrations decrease while OH radicals become more prominent. Elevated OH levels enhance the conversion of NH_2 to NO, prioritizing NO formation over other pathways. This highlights the critical role of OH radicals in NOx production, with even small amounts of ammonia significantly contributing to NOx emissions. For instance, increasing the ammonia ratio from 20% (Case 1) to 30% (Case 2) led to a 14.28% rise in maximum NOx concentrations. The highest NOx levels, including NO, NO_2, and N_2O, were observed at an ammonia concentration of 30% and an equivalence ratio of 0.85.
- During the combustion of ammonia/methane mixtures, NO_2 production is minimal, whereas N_2O makes a significantly larger contribution, particularly at higher equivalence ratios. However, the dominant nitrogen oxide produced is NO. Among all cases studied, the highest observed concentration of N_2O was 1189 PPM, compared to a maximum of 80 PPM for NO_2.

ACKNOWLEDGEMENTS

The authors wish to acknowledge the support established by King Fahd University of Petroleum & Minerals (KFUPM) done by the KFUPM Consortium for Hydrogen Future on project no. H2FC2309. The support received through the KFUPM Interdisciplinary Research Center for Hydrogen Technologies and Carbon Management (IRC-HTCM) on project no. INHT2409 is also appreciated.

REFERENCES

[1]El-Adawy M, Nemitallah MA, Abdelhafez A. Towards sustainable hydrogen and ammonia internal combustion engines:
Challenges and opportunities. Fuel 2024;364:131090.
[2] El-Adawy M, Dalha IB, Ismael MA, Al-Absi ZA, Nemitallah MA. Review of Sustainable Hydrogen Energy Processes:
Production, Storage, Transportation, and Color-Coded Classifications. Energy & Fuels 2024.
[3]Nemitallah MA, Alnazha AA, Ahmed U, El-Adawy M, Habib MA. Review on techno-economics of hydrogen production
using current and emerging processes: Status and perspectives. Results in Engineering 2024:101890.
[4] Ciccarelli G, Jackson D, Verreault J. Flammability limits of NH3–H2–N2–air mixtures at elevated initial temperatures.
Combustion and Flame 2006;144(1-2):53-63.
[5] Mathieu O, Petersen EL. Experimental and modeling study on the high-temperature oxidation of Ammonia and
related NOx chemistry. Combustion and flame 2015;162(3):554-70.
[6] Lee S, Kwon OC. Effects of ammonia substitution on extinction limits and structure of counterflow nonpremixed
hydrogen/air flames. International journal of hydrogen energy 2011;36(16):10117-28.
[7] Li J, Zhang R, Pan J, Wei H, Shu G, Chen L. Ammonia and hydrogen blending effects on combustion stabilities in
optical SI engines. Energy Conversion and Management 2023;280:116827.
[8] Somarathne KDKA, Hatakeyama S, Hayakawa A, Kobayashi H. Numerical study of a low emission gas turbine like
combustor for turbulent ammonia/air premixed swirl flames with a secondary air injection at high pressure. International Journal
of Hydrogen Energy 2017;42(44):27388-99.
[9] Kurata O, Iki N, Inoue T, Matsunuma T, Tsujimura T, Furutani H, et al. Development of a wide range-operable, rich
lean low-NOx combustor for NH3 fuel gas-turbine power generation. Proceedings of the combustion Institute 2019;37(4):4587
95.

[10] da Rocha RC, Costa M, Bai X-S. Chemical kinetic modelling of ammonia/hydrogen/air ignition, premixed flame
propagation and NO emission. Fuel 2019;246:24-33.
[11] Ariemma GB, Sorrentino G, Ragucci R, de Joannon M, Sabia P. Ammonia/Methane combustion: stability and NOx
emissions. Combustion and Flame 2022;241:112071.
[12] Zhang R, Chen L, Wei H, Li J, Ding Y, Chen R, et al. Experimental investigation on reactivity-controlled compression
ignition (RCCI) combustion characteristic of n-heptane/ammonia based on an optical engine. International Journal of Engine
Research 2023;24(6):2478-88.
[13] Valera-Medina A, Marsh R, Runyon J, Pugh D, Beasley P, Hughes T, et al. Ammonia–methane combustion in
tangential swirl burners for gas turbine power generation. Applied Energy 2017;185:1362-71.
[14] Zitouni SE, Mashruk S, Mukundakumar N, Brequigny P, Zayoud A, Pucci E, et al. AMMONIA BLENDED fuels
energy solutions for a green future. *10th International Gas Turbine Conference*. 2021.
[15] El-Adawy M, Hamdy M, Abdelhafez A, Abdelhalim A, Nemitallah MA. Stability and combustion characteristics of
dual annular counter-rotating swirl oxy-methane flames: Effects of equivalence and velocity ratios. Case Studies in Thermal
Engineering 2024;61:104927.
[16] Füzesi D, Wang S, Józsa V, Chong CT. Ammonia-methane combustion in a swirl burner: Experimental analysis and
numerical modeling with Flamelet Generated Manifold model. Fuel 2023;341:127403.
[17] Fu Z, Gao H, Zeng Z, Liu J, Zhu Q. Generation characteristics of thermal NOx in a double-swirler annular combustor
under various inlet conditions. Energy 2020;200:117487.
[18] Okafor EC, Naito Y, Colson S, Ichikawa A, Kudo T, Hayakawa A, et al. Measurement and modelling of the laminar
burning velocity of methane-ammonia-air flames at high pressures using a reduced reaction mechanism. Combustion and Flame
2019;204:162-75.
[19] Liu X, Wang G, Si J, Wu M, Xu M, Mi J. On a premixed NH3/O2 jet flame in hot coflow of gaseous H2O versus N2.
International Journal of Hydrogen Energy 2024;72:588-600.
[20] Sadatakhavi S, Tabejamaat S, EiddiAttarZade M, Kankashvar B, Nozari M. Numerical and experimental study of the
effects of fuel injection and equivalence ratio in a can micro-combustor at atmospheric condition. Energy
2021;225:120166.
[21] Shrestha KP, Lhuillier C, Barbosa AA, Brequigny P, Contino F, Mounaïm-Rousselle C, et al. An experimental and
modeling study of ammonia with enriched oxygen content and ammonia/hydrogen laminar flame speed at elevated pressure and
temperature. Proceedings of the Combustion Institute 2021;38(2):2163-74.
[22] Kobayashi H, Hayakawa A, Somarathne KKA, Okafor EC. Science and technology of ammonia combustion.
Proceedings of the combustion institute 2019;37(1):109-33.
[23] Sabia P, Manna MV, Ragucci R, de Joannon M. Mutual inhibition effect of hydrogen and ammonia in oxidation
processes and the role of ammonia as “strong” collider in third-molecular reactions. International Journal of Hydrogen Energy
2020;45(56):32113-27.